ORIGINAL ARTICLE

Quantification of myocardial blood flow by CZT-SPECT with motion correction and comparison with ^{15}O-water PET

Yuka Otaki, MD, PhD,[a] Osamu Manabe, MD, PhD,[a,b] Robert J. H. Miller, MD,[a] Alain Manrique, MD, PhD,[c] Catherine Nganoa, MD,[c] Nathaniel Roth, MSc,[d] Daniel S. Berman, MD,[a] Guido Germano, PhD,[a] Piotr J. Slomka, PhD,[a] and Denis Agostini, MD, PhD[c]

[a] Departments of Imaging and Medicine, Cedars-Sinai Medical Center, Los Angeles, CA
[b] Department of Nuclear Medicine, Hokkaido University of Graduate School of Medicine, Sapporo, Japan
[c] Department of Nuclear Medicine, CHU Cote de Nacre, Normandy University, Caen, France
[d] Spectrum Dynamics Medical Ltd., Caesarea, Israel

Background. We compared quantification of MBF and myocardial flow reserve (MFR) with a 99mTc-sestamibi CZT-SPECT to ^{15}O-water PET.

Methods. SPECT MBF for thirty patients in the WATERDAY study was re-analyzed by QPET software with motion correction and optimal placement of the arterial input function. ^{15}O-water PET MBF was re-quantified using dedicated software. Inter-operator variability was assessed using repeatability coefficients (RPC).

Results. Significant correlations were observed between global ($r = 0.91$, $P < 0.001$) and regional MBF ($r = 0.86$, $P < 0.001$) with SPECT compared to PET. Global MBF (rest 0.95 vs 1.05 ml/min/g, $P = 0.07$; stress 2.62 vs 2.68 mL/min/g, $P = 0.17$) and MFR (2.65 vs 2.75, $P = 0.86$) were similar between SPECT and PET. Rest (0.81 vs 0.98 mL/min/g, $P = 0.03$) and stress MBF (1.98 vs 2.61 mL/min/g, $P = 0.01$) in right coronary artery (RCA) were lower with SPECT compared to PET. However, MFR in the RCA territory was similar (2.54 vs 2.77, $P = 0.21$). The SPECT-PET RPC for global MBFs and MFR were 0.95 mL/min/g and 0.94, with inter-observer RPC of 0.59 mL/min/g and 0.74, respectively.

Conclusions. MBF and MFR derived from CZT-SPECT with motion correction and optimal placement of the arterial input function showed good agreement with ^{15}O-water PET, as well as low inter-operator variability. (J Nucl Cardiol 2021;28:1477–86.)

Key Words: Myocardial blood flow • single-photon emission computed tomography • positron emission tomography

Abbreviations	
CAD	Coronary artery disease
CZT	Cadmium zinc telluride
MBF	Myocardial blood flow
MFR	Myocardial flow reserve
MPI	Myocardial perfusion imaging
PET	Positron emission tomography
ROI	Region of interest
RPC	Repeatability coefficient
SPECT	Single-photon emission computed tomography

See related editorial, pp. 1487–1489

INTRODUCTION

Myocardial perfusion imaging (MPI) with single-photon emission computed tomography (SPECT) plays an important role in the diagnosis and management of coronary artery disease (CAD), with 7-8 million scans performed annually in the United States.[1] SPECT quantification of ischemia as a regional perfusion deficit has important prognostic value.[2,3] However, SPECT MPI is inherently insensitive to balanced ischemia due to left main disease or triple-vessel disease.[4]

Myocardial blood flow (MBF), which was initially estimated with positron emission tomography (PET), increases diagnostic accuracy for obstructive CAD,[5] and improves prediction of adverse cardiovascular events compared to regional perfusion alone.[6] While MBF obtained with PET is considered a gold standard, the potential clinical impact of measuring MBF with SPECT is high, since SPECT is used more widely than cardiac PET—representing over 95% of MPI.[7] Cadmium zinc telluride (CZT) SPECT camera systems have higher photon sensitivity compared to conventional Anger cameras,[8,9] which facilitate MBF measurements from early dynamic acquisitions.[10–16]

We recently adapted QPET algorithms (Cedars-Sinai Medical Center) to quantify dynamic SPECT data, which also allows for motion correction and optimal positioning of the arterial input function (AIF). The aim of this study was to evaluate the quantification and inter-observer variability of MBF and MFR with a CZT-SPECT camera, utilizing this new algorithm compared to ^{15}O-water PET results using the WATERDAY study image dataset.[10]

METHODS

Study Subjects

Details of the study population and the study protocol have been described previously.[10] Briefly, from November 2014 to November 2016, 104 stable patients with positive exercise stress test or perfusion imaging who were referred for invasive angiography were screened for WATER DAY trial (clinicaltrials.gov unique identifier NCT02278497). Among these patients, 45 patients with angiography-proven CAD and fractional flow reserve (FFR) measurements were enrolled in the trial. Thirty out of 45 patients underwent ^{99m}Tc-sestamibi SPECT and ^{15}O-water PET within 30 days and are included in the current study. The study protocol was approved by the Regional Ethics Committee (CPP Nord-Ouest lll, France), written informed consent was obtained from all the patients, and the procedures were in accordance with the Declaration of Helsinki.

Dynamic ^{99m}Tc-sestamibi CZT-SPECT Acquisition Protocol

Rest and stress dynamic images were acquired in list mode over 6 minutes. For rest imaging, approximately 37 MBq of ^{99m}Tc-sestamibi was used to position the patient's heart within the field of view.[17] Three MBq/kg was injected at a rate of 1-2 cm^3/s using an automatic injector (Nemoto, Tokyo, Japan) and flushed by 30 mL of saline to ensure consistent delivery of a tight bolus. For stress imaging, 9 MBq/kg of ^{99m}Tc-sestamibi was injected after the administration of regadenoson (400 µg). Rest-stress dynamic acquisitions were completed within 75 min. Data were rebinned into 32 frames consisting of 21×3, 1×9, 1×15, 1×21, 1×27 and 7×30-seconds frames. An ordered subset expectation maximization (OSEM) algorithm was used for image reconstruction with 4 iterations and 32 subsets.

MBF Quantification by Dynamic ^{99m}Tc-Sestamibi CZT-SPECT

A global myocardial region of interest (ROI) was placed semi-automatically to obtain the myocardial time activity curves from the summed dynamic image data, starting 2 minutes after the last frame images of the dynamic SPECT data.[18] First, MBF was automatically derived by the software without motion correction and with the AIF positioned in the center of the LV cavity along the mitral valve.[19] The 3D cylindrical region of interest (ROI) used for AIF extraction was automatically set in the LV cavity based on early uptake images, using a cube oriented along the long axis of the heart.[19] Subsequently, operators manually corrected the motion effect on each set of dynamic frames and placed the 3D cylindric ROI, avoiding the overlap with the myocardial wall, in the center of left atrium (LA) cavity on the early frame images to obtain the AIF (Figure 1). For each frame in each dataset, two operators (Y.O. and O.M) shifted the ROIs in the short-axis, horizontal long-axis, and vertical long-axis images in each of the 3-coordinate axes (x, y, z). The ^{99m}Tc-sestamibi model used a one-tissue compartment model with $k2$ set to 0 (equivalent to net retention model)[20] with blood-to-myocardium spillover fraction and myocardial partial-volume corrections.[21] MBF is obtained by correcting the $K1$ values for the flow-dependent extraction fraction based on the model by

Leppo et al.[20] Regional analysis was performed with standardized myocardial wall segmentation for the left anterior descending (LAD), left circumflex (LCX), and right coronary artery (RCA).[22] Two operators independently performed MBF quantification by dynamic 99mTc-sestamibi CZT-SPECT using motion correction and optimal AIF placement. The operators were blinded to clinical information, PET MBF results, and SPECT MBF results quantified by the other operator, with all analyses performed in a random order.

Dynamic ¹⁵O-Water PET Acquisition Protocol

Participants were instructed to fast for 4 hours and abstain from caffeine, theophylline, and cigarette smoking for 24 hours. All PET acquisitions were performed using a GE Discovery VCT RX (GE Healthcare, Buc, France). After a low-dose transmission CT scan for attenuation correction (AC; helical coverage: 40 mm, rotation time: 0.5 seconds, pitch 0.516:1, table speed: 20.62 mm/rot, helical thickness: 3.75 mm, 120 kV and 10 mA, leading to a DLP of 15.35 mGy.cm and a radiation exposure of 0.21 mSv in all patients), a hand injection of ¹⁵O-water (1.5 to 3 MBq/kg) was performed at rest simultaneously with rest image acquisition. Pharmacological stress was induced by a bolus injection of regadenoson (400

µg), followed by a hand injection of ¹⁵O-water (1.5 to 3 MBq/kg) for the stress scan. PET scans were executed in 3 dimensional (3D) dynamic mode with a 24-frame (14 × 5, 3 × 10, 3 × 20 and 4 × 30 seconds).

MBF Quantification by ¹⁵O-Water PET Image Analysis

Emission sinograms were corrected for random coincidences and dead time after Fourier rebinning and then reconstructed with the PET manufacturer's attenuation and scatter correction using filtered back projection (Hanning filter, cutoff 8 mm). MBF values for ¹⁵O-water PET were requantified using dedicated software (Carimas, Turuk, Finland)[23] for the current study analysis, blinded to the results obtained for the WATERDAY study. Briefly, ROIs were drawn over the global left ventricle (LV) myocardium automatically. The ROI for AIF was placed in the center of LA cavity on the early uptake images. For each frame in each dataset, operators shifted the ROIs in the short-axis, horizontal long-axis, and vertical long-axis images in each of the 3-coordinate axes (x, y, z). Arterial and myocardial tissue activity curves were derived and were fitted to a single-tissue-compartment tracer kinetic model to calculate MBF for the global LV and for each coronary territory.
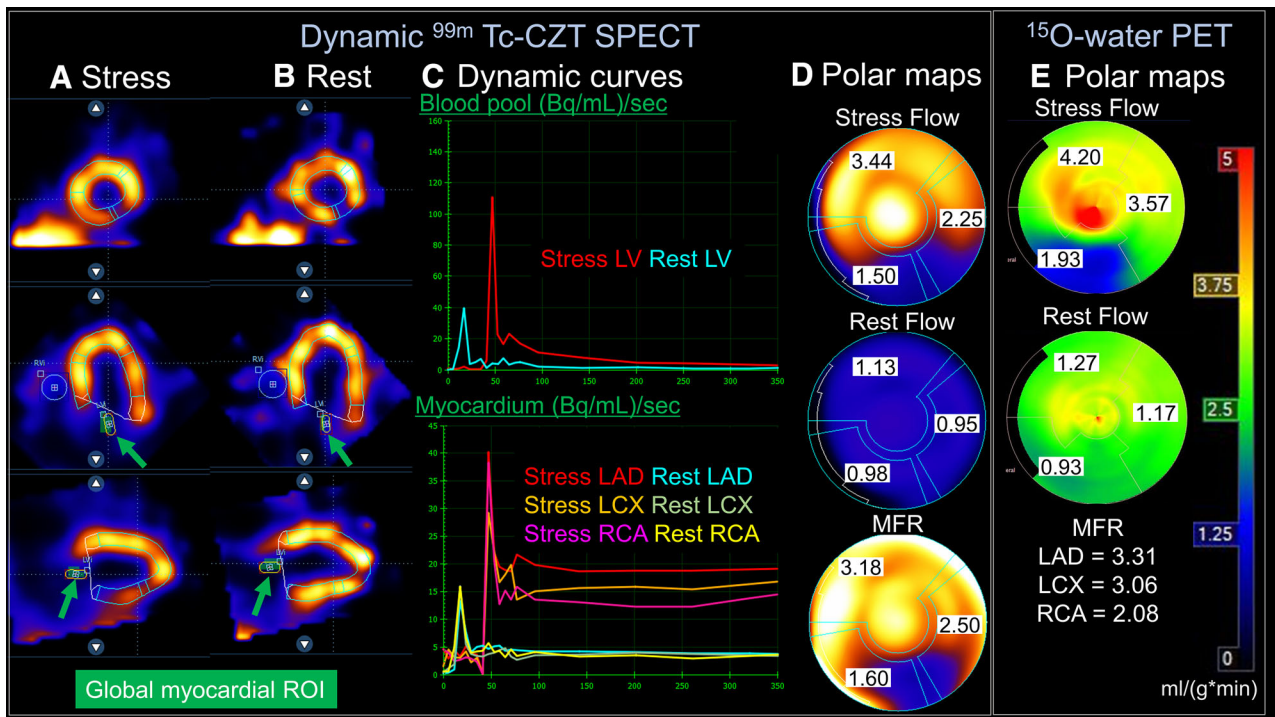
Figure 1. MBF quantification using dynamic ⁹⁹ᵐTc-CZT-SPECT. SPECT images at stress (**A**), and rest (**B**) showing a fixed regional perfusion deficit in the infero-basal segment. Global myocardial ROI are shown as green circles. Dynamic curves of blood pool and myocardium (**C**) and polar maps (**D**) demonstrate decreased stress myocardial blood flow in the RCA distribution which was confirmed with and ¹⁵O-water PET imaging (**E**).

Table 1. Population characteristics

(*n* = 30)	*n* (frequency %)
Male gender	21 (70%)
Mean age ± SD (years)	65 ± 7.1
CAD risk factors	
BMI > 30	8 (27%)
Diabetes mellitus	10 (33%)
Hypertension	20 (67%)
Dyslipidemia	18 (60%)
Smoking history	17 (57%)
Family history	7 (23%)
>3 CAD risk factors	15 (50%)
Chest pain	15 (50%)
Medical therapy	
Clopidogrel	4 (13%)
Aspirin	30 (100%)
β-blocker	18 (60%)
ACE inhibitor or AT-II antagonist	17 (57%)
Calcium channel blocker	6 (20%)
Coumadin	2 (7%)
Statin	25 (83%)
Oral hypoglycemic agent	12 (40%)
Long acting nitrate	6 (20%)
Diuretic	3 (10%)
Insulin	3 (10%)

ACE, inhibitor, angiotensin-converting-enzyme inhibitor; *AT-II* antagonist, angiotensin receptor blocker; *BMI,* Body Mass Index; *CAD,* coronary artery disease; *SD,* standard deviation

Statistical Analysis

Continuous variables are presented as median values with interquartile range (IQR). Categorical variables are presented as absolute numbers with percentages. The correlation of MBF values between SPECT and PET were assessed using linear regression analyses and Bland–Altman plots with calculation of the repeatability coefficient (RPC = 1.96 × standard deviation [SD] of differences). Pearson's correlation coefficients were used to evaluate the concordance between the MBF values obtained at each acquisition. Mann–Whitney *U* test or Wilcoxon signed-rank test was used for intra-group comparisons as appropriate. Receiver-operating-characteristic (ROC) curve analysis was performed to evaluate the ability of SPECT-MFR quantification, with motion correction and optimal placement of the AIF, to predict reduced PET-regional MFR (< 2.0 and < 1.5). Optimal thresholds of SPECT-regional MFR to predict reduced PET-regional MFR were established using the Youden index. A two-tailed *P* value of less than 0.05 was required for statistical significance. Statistical calculations were carried out using SAS (JMP version 13, SAS Institute, Cary, NC, USA).

RESULTS

Hemodynamic Data on SPECT and PET Acquisitions

In total, 30 patients were included with population characteristics outlined in Table 1. The hemodynamic data from SPECT and PET acquisitions are presented in Table 2. There were no significant differences in any of the hemodynamic data, including heart rate, systolic blood pressure, diastolic blood pressure, and rate

Table 2. Hemodynamic data during CZT-SPECT and PET acquisitions

	CZT-SPECT	PET	*P* value
Rest			
HR (bpm)	64.3 ± 12.3	65.5 ± 13.2	0.23
SBP (mmHg)	123.9 ± 21.3	125.2 ± 20.0	0.20
DBP (mmHg)	64.1 ± 10.5	61.7 ± 7.8	0.06
RPP (bpm × mmHg)	7936.9 ± 1755.2	7865.9 ± 1691.8	0.22
Stress			
HR (bpm)	82.0 ± 20.1	80.15 ± 20.3	0.28
SBP (mmHg)	131.03 ± 22.7	130.20 ± 18.3	0.37
DBP (mmHg)	64.3 ± 12.5	61.2 ± 9.1	0.07
RPP (bpm × mmHg)	11074.6 ± 3043.7*	9741.2 ± 4136.9**	0.26

Values are shown as mean ± SD
DBP, diastolic blood pressure; *HR,* heart rate; *RPP,* rate pressure product; *SBP,* systolic blood pressure
*$P = 0.0004$ (rest RPP vs stress RPP) on SPECT
**$P = 0.001$ (rest RPP vs stress RPP) on PET

Table 3. Comparisons in MBF and MFR between CZT-SPECT and PET

		CZT-SPECT	PET	*P* value
Rest MBF (mL/min/g)	Global	0.95 (0.80-1.06)	1.05 (0.85-1.20)	0.07
	LAD	1.00 (0.84-1.17)	1.12 (0.86-1.29)	0.14
	LCX	0.89 (0.76-1.08)	1.08 (0.91-1.26)	**0.01**
	RCA	0.81 (0.68-0.92)	0.98 (0.73-1.08)	**0.03**
Stress MBF (mL/min/g)	Global	2.62 (1.87-2.91)*	2.68 (1.94-3.67)*	0.17
	LAD	2.66 (1.86-3.08)*	2.62 (2.00-3.76)*	0.52
	LCX	2.40 (1.82-2.86)*	2.65 (2.27-3.59)*	0.15
	RCA	1.98 (1.44-2.76)*	2.61 (1.99-3.60)*	**0.01**
MFR	Global	2.65 (2.10-3.21)	2.75 (2.03-3.37)	0.86
	LAD	2.54 (2.11-3.30)	2.56 (1.85-3.24)	0.71
	LCX	2.78 (2.17-3.19)	2.72 (2.10-3.20)	0.80
	RCA	2.54 (1.96-3.32)	2.77 (2.20-3.55)	0.21

P values showing significant differences are shown in bold
Values are shown as median (interquartile range)
CZT, cadmium zinc telluride; *LAD*, left anterior descending coronary artery; *LCX*, left circumflex coronary artery; *MBF*, myocardial blood flow; *MFR*, myocardial flow reserve; *PET*, positron emission tomography; *RCA*, right coronary artery; *SPECT*, single-photon emission computed tomography
*$P < 0.0001$ vs Rest MBF

pressure product (RPP) between SPECT and PET data acquisitions.

MBF Quantification by ^{99m}Tc-Sestamibi CZT-SPECT and ^{15}O-Water PET MBF

Table 3 compares MBF and MFR measurements between SPECT and PET. Global MBF at rest and stress, and both global and regional MFR were similar between SPECT and PET (P for all = not significant). Regional MBF was also similar in the LAD and LCX territories at stress and LAD territory at rest, while it was underestimated by SPECT in the RCA territory at stress ($P = 0.01$) and the LCX ($P = 0.01$) and RCA territories ($P = 0.03$) at rest.
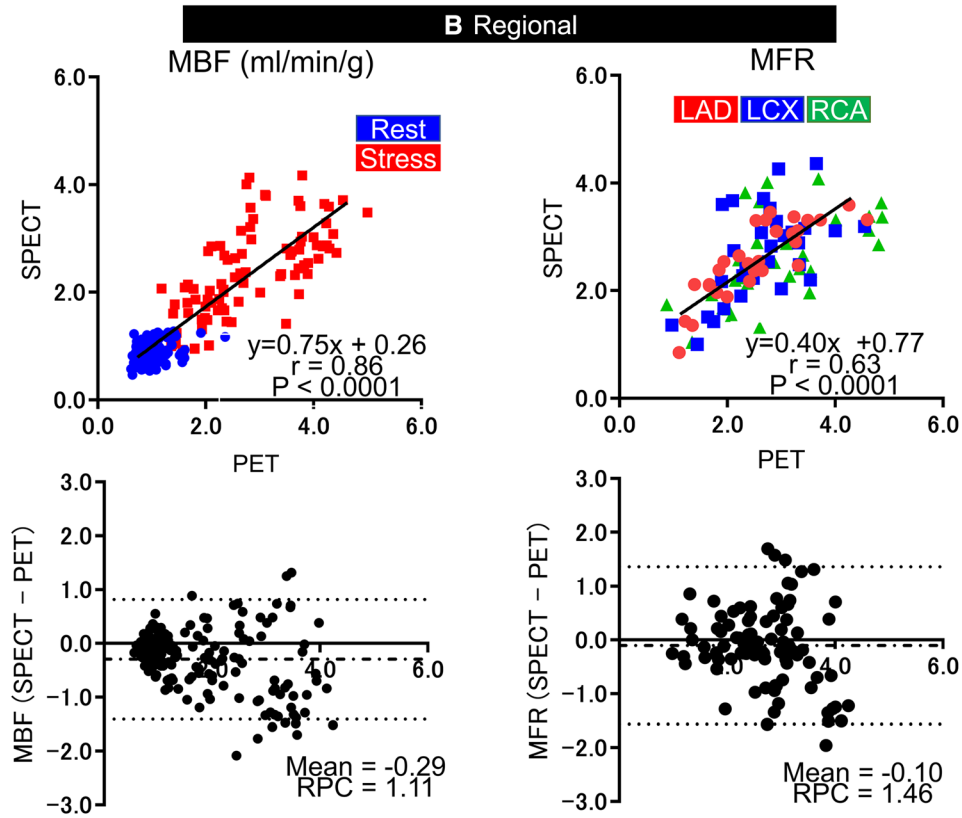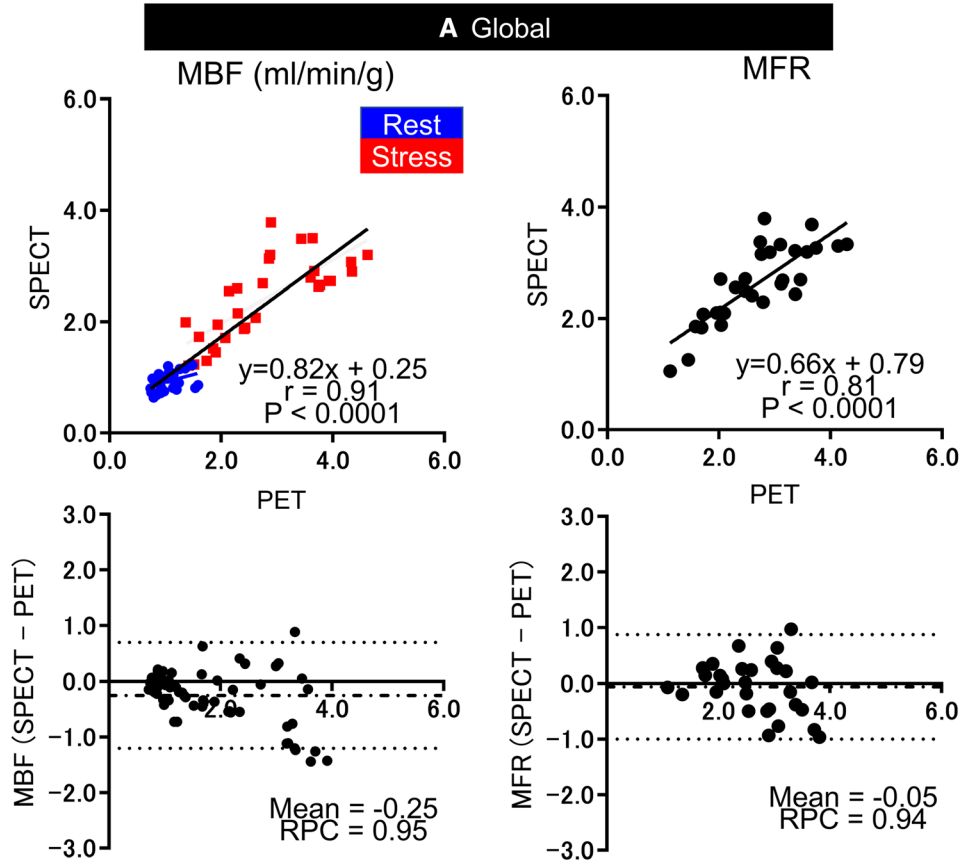
Figure 2 shows correlation and Bland–Altman plots of MBF and MFR between CZT-SPECT and PET. The global MBF ($r = 0.91$, $P < 0.001$) and MFR ($r = 0.81$, $P < 0.001$) values obtained from CZT-SPECT correlated well with those obtained from ^{15}O-water PET (Figure 2a). RPC for global MBF was 0.95 mL/min/g and 0.94 for global MFR. The regional MBF ($r = 0.86$, $P < 0.001$) and MFR ($r = 0.63$, $P < 0.001$) values by CZT-SPECT also correlated well with PET measurements (Figure 2b). RPC for regional estimation was 1.11 mL/min/g for MBF and 1.46 for MFR. The motion correction and optimal placement of the arterial input function was performed for dynamic SPECT data at stress and rest in all 30 patients. The fraction of stress studies that required motion correction ≥ 5 mm in any axes and any frames was similar to rest studies (Stress:

93% vs Rest: 83%, $P = 0.23$). Global and regional MBF by CZT-SPECT demonstrated comparatively worse correlation with ^{15}O-Water PET measurements if only optimal AIF was placed and motion correction was not performed ($r = 0.65$, $P < 0.0001$ for global estimates and $r = 0.63$, $P < 0.0001$ for regional estimates). The MBF after MC decreased from 2.54 ± 0.84 to 2.36 ± 0.83 mL/g/min at stress ($P = 0.14$) and from 0.99 ± 0.19 to 0.91 ± 0.21 mL/g/min at rest ($P = 0.001$).

ROC analysis per regional analysis demonstrated that the AUC of SPECT-regional MFR with motion correction and optimal placement of the AIF was 0.89 [0.79-0.98] for the detection of PET-regional MFR < 2.0, and 0.96 [0.91-1.00] for the detection of PET-regional MFR < 1.5. Optimal cutoffs of SPECT-regional MFR were 2.18 for the detection of PET-regional MFR < 2.0 (sensitivity 85.0 %, specificity 87.1%) and 2.13 for the detection of PET-regional MFR < 1.5 (sensitivity 100.0%, specificity 81.7%).

Inter-operator Variability of CZT-SPECT

Figure 3 shows correlation and Bland–Altman plots for global and regional MBF and MFR by CZT-SPECT between two operators. The plots demonstrate high correlation coefficients for global ($r = 0.95$ for MBF and $r = 0.86$ for MFR) and regional estimates ($r = 0.93$ for MBF and $r = 0.82$ for MFR). RPC for global MBF was 0.59 ml/min/g and 0.70 ml/min/g for regional MBF

A Global

MBF (ml/min/g)
Rest
Stress
y=0.82x + 0.25
r = 0.91
P < 0.0001

MFR
y=0.66x + 0.79
r = 0.81
P < 0.0001

Mean = -0.25
RPC = 0.95

Mean = -0.05
RPC = 0.94

B Regional

MBF (ml/min/g)
Rest
Stress
y=0.75x + 0.26
r = 0.86
P < 0.0001

MFR
LAD LCX RCA
y=0.40x + 0.77
r = 0.63
P < 0.0001

Mean = -0.29
RPC = 1.11

Mean = -0.10
RPC = 1.46

◀**Figure 2.** Correlation between CZT-SPECT and ^{15}O-water PET. Correlation and Bland–Altman analyses of SPECT compared to PET MBF and MFR measurements for global (**A**) and regional (**B**) values. *CZT*, cadmium zinc telluride; *LAD*, left anterior descending coronary artery; *LCX*, left circumflex coronary artery; *MBF*, myocardial blood flow; *MFR*, myocardial flow reserve; *PET*, positron emission tomography; *RCA*, right coronary artery; *RPC*, repeatability coefficient; *SPECT*, single-photon emission computed tomography.

estimation, while RPC for MFR was 0.74 for global estimates and 0.99 for regional estimates.

DISCUSSION

In this study, we have shown the feasibility of MBF quantification from CZT-SPECT using a new PET-based software application. We were able to adjust SPECT MBF measurements for the extraction fraction of ^{99m}Tc, with motion correction and optimal placement of the AIF. We show that both MBF and MFR values correlated well with ^{15}O-water PET and demonstrated high inter-operator reproducibility. In addition, the sensitivity and specificity of CZT-SPECT MFR for the detection of reduced PET-MFR were excellent. Lastly, the optimal thresholds for detection of reduced regional MFR by PET in our study (2.18 for PET-MFR < 2.0 and 2.13 for PET-MFR < 1.5) were similar to the thresholds for CZT-SPECT MFR to predict abnormal FFR reported in the WATERDAY study (cutoff 2.1).[10]

Multiple reports have demonstrated the feasibility of SPECT MBF quantification.[10–16,24–27] Two studies have performed head-to-head comparisons between SPECT with a CZT camera system and PET. Nkoulo et al studied 28 patients who underwent ^{99m}Tc-tetrofosmin CZT-SPECT and ^{13}N-ammonia PET using the PMOD software package (PMOD technologies Ltd, Zurich, Switzerland).[15] There was moderate correlation, assessed using Spearman's correlation, between SPECT and PET for stress ($\rho = 0.51$, $P < 0.001$) and rest ($\rho = 0.30$, $P =$ not significant) measurements. Stress MBF was underestimated by SPECT at high flow conditions, resulting in underestimation of MFR. However, the authors did not correct for the extraction fraction of ^{99m}Tc, which is a significant limitation of SPECT MBF measurements, particularly at high flows. The WATERDAY study compared MBF quantification between ^{99m}Tc-sestamibi CZT-SPECT and ^{15}O-water PET. They demonstrated good correlation in MBF and MFR between SPECT and PET using Corridor 4DM software (INVIA, Ann Arbor, MI, USA).[10] Correlation coefficients between SPECT and PET were $r = 0.83$ for

MBF ($P < 0.001$) and $r = 0.75(P < 0.001)$ for MFR, with a mean difference of 0.33 for MBF and 0.13 for MFR.[10] In contrast to results from Nkoulo et al, global stress MBF by ^{99m}Tc-sestamibi CZT-SPECT was higher compared to ^{15}O-water PET values. In the same population as the WATERDAY study but with different software, we demonstrated slightly better correlation between SPECT and PET MBF ($r = 0.91$ vs $r = 0.83$) and MFR ($r = 0.81$ vs $r = 0.75$) with no significant differences in global MBF or MFR measurements between SPECT and PET. Our results provide critical external validation of the WATERDAY results, by demonstrating similar results with new software and different observers. These findings suggest that comparable measurements of MBF with PET and SPECT can be obtained by integrating corrections for extraction fraction with motion correction and optimal AIF placement. Previous studies have shown that myocardial spillover contamination of arterial input in the LV cavity was higher compared with the LA using ^{15}O-water and nitrogen-13 ammonia PET.[28,29] In a different study, Vasquez et al assessed MBF quantification using various anatomic arterial inputs.[30] They demonstrated that rest MBF in the LV cavity was higher than in the aorta or LA, while rest MBF in the LA was not significantly different from that in the aorta. These previous PET studies have shown that MBF quantification with positioning of the AIF to the left atrium is more accurate and reproducible.

While our global measurements of MBF and MFR were comparable between SPECT and PET, we demonstrated important regional differences. Rest MBF measurements were lower in the RCA and LCX territories by SPECT compared to PET and stress MBF was lower in the RCA territory. Interestingly, the WATERDAY study found higher SPECT MBF values at rest and stress in the LAD and LCX territories, but not the RCA. This may be due to the differences in software methods. Attenuation artifacts with CZT-SPECT camera systems are more common in the inferolateral and lateral wall,[31] which may impact MBF measurements in these territories. Wells et al demonstrated that CT attenuation correction improved the correlation between regional MBF by SPECT compared to PET, but led to worse correlation with global values.[11] Therefore, attenuation correction may be particularly beneficial for the RCA and LCX territories, but does not seem to be necessary when considering global measurements.

Multiple previous PET studies have shown that patient motion is problematic for MBF measurement.[32,33] Wells et al have reported that motion correction improved the accuracy and precision of global and regional SPECT MBF measurements compared with PET.[11] In the current study, two operators
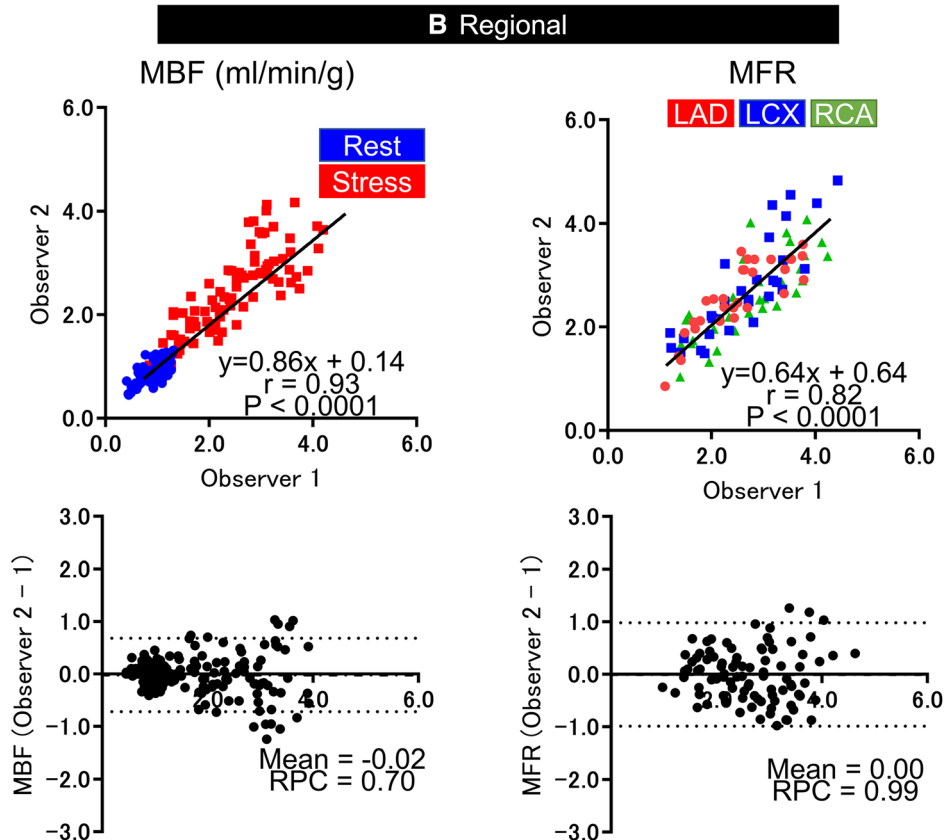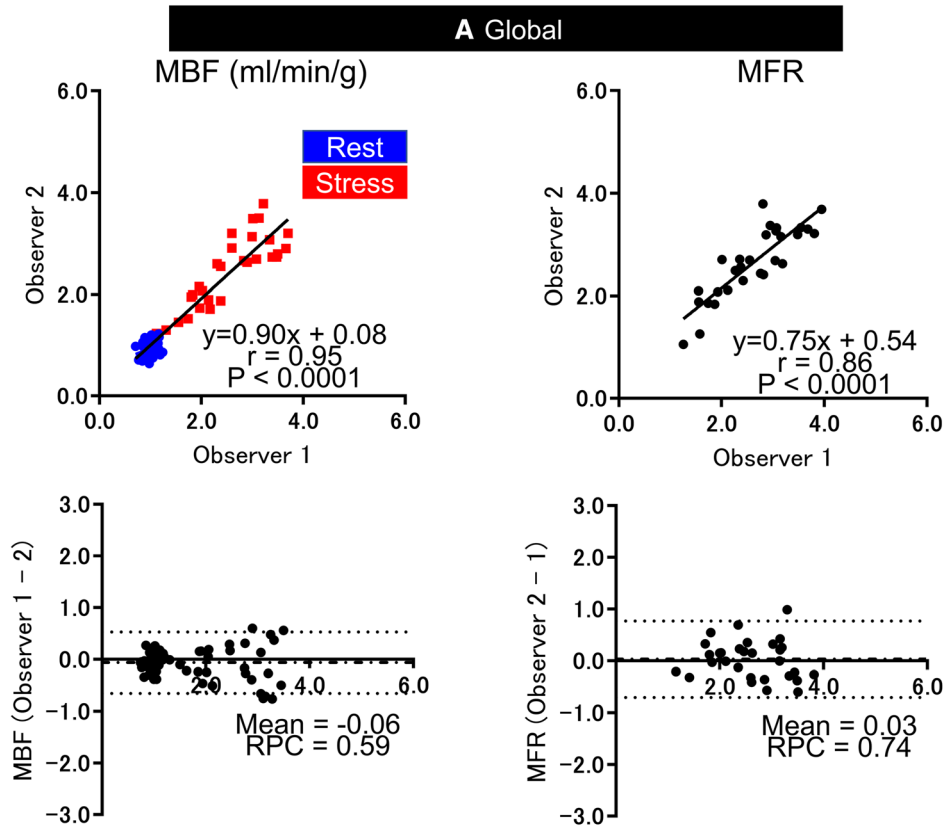
◄**Figure 3.** Inter-operator variability in MBF and MFR quantification by 99mTc-dynamic CZT-SPECT. Correlation and Bland–Altman analyses in MBF and MFR measurements for global (**A**) and regional (**B**) values between two observers. *CZT*, cadmium zinc telluride; *LAD*, left anterior descending coronary artery; *LCX*, left circumflex coronary artery; *MBF*, myocardial blood flow; *MFR*, myocardial flow reserve; *PET*, positron emission tomography; *RCA*, right coronary artery; *RPC*, repeatability coefficient; *SPECT*, single-photon emission computed tomography.

independently corrected motion using a semi-automated program which resulted in good correlation in for global ($r = 0.95$ for MBF, $r = 0.86$ for MFR) and regional estimates ($r = 0.93$ for MBF, $r = 0.82$ for MFR). Our results build upon the prior data demonstrating the importance of motion correction by comparing to ^{15}O-water PET, the gold standard for non-invasive MBF measurement.[34–36] Additionally, our semi-automated approach may help decrease result variability, which may be particularly important for patients with serial testing.

LIMITATIONS

Our study has a few important limitations. The sample size was relatively small, but still demonstrates the feasibility of SPECT MBF measurements with the PET-based software. Attenuation correction has not been used, but previous studies have shown that attenuation correction does not significantly change global MBF measurements. Lastly, SPECT measurements were performed with a CZT camera system, which are not yet widely used; however, there are over 800 of these systems currently installed worldwide and most cardiac replacement cameras are solid state.

NEW KNOWLEDGE GAINED

Dynamic ^{99m}Tc-sestamibi CZT-SPECT allows MBF and MFR quantification, which correlate well with ^{15}O-water values. There was close inter-operator correlation in MBF and MFR for global and regional estimations using this semi-automated approach.

CONCLUSIONS

Our quantitative method demonstrated a good correlation in MBF and MFR between ^{99m}Tc-sestamibi CZT-SPECT and ^{15}O-water PET with high inter-operator reproducibility.

References

1. Chen J. The frontiers of nuclear cardiology research. J Biomed Res 2013;27:437-8.
2. Berman DS, Hachamovitch R, Kiat H, Cohen I, Cabico JA, Wang FP, et al. Incremental value of prognostic testing in patients with known or suspected ischemic heart disease: A basis for optimal utilization of exercise technetium-99m sestamibi myocardial perfusion single-photon emission computed tomography. J Am Coll Cardiol 1995;26:639-47.
3. Hachamovitch R, Berman DS, Kiat H, Cohen I, Cabico JA, Friedman J, et al. Exercise myocardial perfusion SPECT in patients without known coronary artery disease: incremental prognostic value and use in risk stratification. Circulation 1996;93:905-14.
4. Berman DS, Kang X, Slomka PJ, Gerlach J, de Yang L, Hayes SW, et al. Underestimation of extent of ischemia by gated SPECT myocardial perfusion imaging in patients with left main coronary artery disease. J Nucl Cardiol 2007;14:521-8.
5. Yoshinaga K, Katoh C, Manabe O, Klein R, Naya M, Sakakibara M, et al. Incremental diagnostic value of regional myocardial blood flow quantification over relative perfusion imaging with generator-produced rubidium-82 PET. Circ J 2011;75:2628-34.
6. Farhad H, Dunet V, Bachelard K, Allenbach G, Kaufmann PA, Prior JO. Added prognostic value of myocardial blood flow quantitation in rubidium-82 positron emission tomography imaging. Eur Heart J Cardiovasc Imaging 2013;14:1203-10.
7. Levin DC, Parker L, Halpern EJ, Rao VM. Recent trends in imaging for suspected coronary artery disease: What is the best approach? J Am Coll Radiol 2016;13:381-6.
8. Sharir T, Ben-Haim S, Merzon K, Prochorov V, Dickman D, Ben-Haim S, et al. High-speed myocardial perfusion imaging: Initial clinical comparison with conventional dual detector anger camera imaging. JACC Cardiovasc Imaging 2008;1:156-63.
9. Imbert L, Poussier S, Franken PR, Songy B, Verger A, Morel O, et al. Compared performance of high-sensitivity Cameras dedicated to myocardial perfusion SPECT: A comprehensive analysis of phantom and human images. J Nucl Med 2012;53:1897-903.
10. Agostini D, Roule V, Nganoa C, Roth N, Baavour R, Parienti JJ, et al. First validation of myocardial flow reserve assessed by dynamic (99m)Tc-sestamibi CZT-SPECT camera: head to head

comparison with (15)O-water PET and fractional flow reserve in patients with suspected coronary artery disease. The WATERDAY study. Eur J Nucl Med Mol Imaging 2018;45:1079-90.

11. Wells RG, Marvin B, Poirier M, Renaud J, deKemp RA, Ruddy TD. Optimization of SPECT measurement of myocardial blood flow with corrections for attenuation, motion, and blood binding compared with PET. J Nucl Med 2017;58:2013-9.

12. Ben-Haim S, Murthy VL, Breault C, Allie R, Sitek A, Roth N, et al. Quantification of myocardial perfusion reserve using dynamic SPECT imaging in humans: A feasibility study. J Nucl Med 2013;54:873-9.

13. Han S, Kim YH, Ahn JM, Kang SJ, Oh JS, Shin E, et al. Feasibility of dynamic stress (201)Tl/rest (99m)Tc-tetrofosmin single photon emission computed tomography for quantification of myocardial perfusion reserve in patients with stable coronary artery disease. Eur J Nucl Med Mol Imaging 2018;45:2173-80.

14. Ma R, Wang L, Wu D, Wang M, Sun X, Hsu B, et al. Myocardial blood flow quantitation in patients with congestive heart failure: head-to-head comparison between rapid-rotating gantry SPECT and CZT SPECT. J Nucl Cardiol 2019. https://doi.org/10.1007/s12350-019-01621-2.

15. Nkoulou R, Fuchs TA, Pazhenkottil AP, Kuest SM, Ghadri JR, Stehli J, et al. Absolute myocardial blood flow and flow reserve assessed by gated SPECT with cadmium-zinc-telluride detectors using 99mTc-tetrofosmin: Head-to-head comparison with 13N-ammonia PET. J Nucl Med 2016;57:1887-92.

16. Ben Bouallegue F, Roubille F, Lattuca B, Cung TT, Macia JC, Gervasoni R, et al. SPECT myocardial perfusion reserve in patients with multivessel coronary disease: correlation with angiographic findings and invasive fractional flow reserve measurements. J Nucl Med 2015;56:1712-7.

17. Bellevre D, Manrique A, Legallois D, Bross S, Baavour R, Roth N, et al. First determination of the heart-to-mediastinum ratio using cardiac dual isotope ((1)(2)(3)I-MIBG/(9)(9)mTc-tetrofosmin) CZT imaging in patients with heart failure: the ADRECARD study. Eur J Nucl Med Mol Imaging 2015;42:1912-9.

18. Germano G, Kavanagh PB, Chen J, Waechter P, Su HT, Kiat H, et al. Operator-less processing of myocardial perfusion SPECT studies. J Nucl Med 1995;36:2127-32.

19. Dekemp RA, Declerck J, Klein R, Pan XB, Nakazato R, Tonge C, et al. Multisoftware reproducibility study of stress and rest myocardial blood flow assessed with 3D dynamic PET/CT and a 1-tissue-compartment model of 82Rb kinetics. J Nucl Med 2013;54:571-7.

20. Leppo JA, Meerdink DJ. Comparison of the myocardial uptake of a technetium-labeled isonitrile analogue and thallium. Circ Res 1989;65:632-9.

21. Nesterov SV, Deshayes E, Sciagra R, Settimo L, Declerck JM, Pan XB, et al. Quantification of myocardial blood flow in absolute terms using (82)Rb PET imaging: the RUBY-10 Study. JACC Cardiovasc Imaging 2014;7:1119-27.

22. Cerqueira MD, Weissman NJ, Dilsizian V, Jacobs AK, Kaul S, Laskey WK, et al. Standardized myocardial segmentation and nomenclature for tomographic imaging of the heart. Circulation 2002;105:539-42.

23. Nesterov SV, Han C, Maki M, Kajander S, Naum AG, Helenius H, et al. Myocardial perfusion quantitation with 15O-labelled water

PET: High reproducibility of the new cardiac analysis software (Carimas). Eur J Nucl Med Mol Imaging 2009;36:1594-602.

24. Shrestha U, Sciammarella M, Alhassen F, Yeghiazarians Y, Ellin J, Verdin E, et al. Measurement of absolute myocardial blood flow in humans using dynamic cardiac SPECT and 99mTc-tetrofosmin: Method and validation. J Nucl Cardiol 2015;24:268-77.

25. Hsu B, Chen F-C, Wu T-C, Huang W-S, Hou P-N, Chen C-C, et al. Quantitation of myocardial blood flow and myocardial flow reserve with 99mTc-sestamibi dynamic SPECT/CT to enhance detection of coronary artery disease. Eur J Nucl Med Mol Imaging 2014;41:2294-306.

26. Klein R, Hung G, Wu T, Huang W, Li D, DeKemp R, et al. Feasibility and operator variability of myocardial blood flow and reserve measurements with 99mTc-Sestamibi quantitative dynamic SPECT/CT imaging. J Nucl Cardiol 2014;21:1075-88.

27. Wells RG, Timmins R, Klein R, Lockwood J, Marvin B, deKemp RA, et al. Dynamic SPECT measurement of absolute myocardial blood flow in a porcine model. J Nucl Med 2014;55:1685-91.

28. Hove JD, Iida H, Kofoed KF, Freiberg J, Holm S, Kelbaek H. Left atrial versus left ventricular input function for quantification of the myocardial blood flow with nitrogen-13 ammonia and positron emission tomography. Eur J Nucl Med Mol Imaging 2004;31:71-6.

29. Iida H, Rhodes CG, de Silva R, Araujo LI, Bloomfield PM, Lammertsma AA, et al. Use of the left ventricular time-activity curve as a noninvasive input function in dynamic oxygen-15-water positron emission tomography. J Nucl Med 1992;33:1669-77.

30. Vasquez AF, Johnson NP, Gould KL. Variation in quantitative myocardial perfusion due to arterial input selection. JACC Cardiovasc Imaging 2013;6:559-68.

31. Oddstig J, Martinsson E, Jogi J, Engblom H, Hindorf C. Differences in attenuation pattern in myocardial SPECT between CZT and conventional gamma cameras. J Nucl Cardiol 2018. https://doi.org/10.1007/s12350-018-1296-6.

32. Hunter CR, Klein R, Beanlands RS, deKemp RA. Patient motion effects on the quantification of regional myocardial blood flow with dynamic PET imaging. Med Phys 2016;43:1829.

33. Hunter C, Klein R, Alessio AM, deKemp RA. Patient body motion correction for dynamic cardiac PET-CT by attenuation-emission alignment according to projection consistency conditions. Med Phys 2019;46:1697-706.

34. Bergmann SR, Herrero P, Markham J, Weinheimer CJ, Walsh MN. Noninvasive quantitation of myocardial blood flow in human subjects with oxygen-15-labeled water and positron emission tomography. J Am Coll Cardiol 1989;14:639-52.

35. Driessen RS, Danad I, Stuijfzand WJ, Schumacher SP, Knuuti J, Maki M, et al. Impact of revascularization on absolute myocardial blood flow as assessed by serial [(15)O]H$_2$O positron emission tomography imaging: A comparison with fractional flow reserve. Circ Cardiovasc Imaging 2018;11:e007417.

36. Danad I, Raijmakers PG, Appelman YE, Harms HJ, de Haan S, van den Oever ML, et al. Hybrid imaging using quantitative H$_2^{15}$O PET and CT-based coronary angiography for the detection of coronary artery disease. J Nucl Med 2013;54:55-63.